WIND POWER INVERTER CONTROL OF DC BUS VOLTAGE BASED ON LADRC WITH INTELLIGENT CONTROLLERS

RAJAM MAHENDRA DHARANI[1], Smt. M. NAGA CHAITRA[2], Smt. P. SWATHI[3]

[1]PG-Scholar, Department of EEE (Electrical Power Systems), JNTUA College of Engineering, Ananthapuramu, A.P., India.

[2]Assistant Professor (Adhoc), Department of EEE, JNTUA College of Engineering, Ananthapuramu., A.P., India.

[3]Assistant Professor (Adhoc), Department of EEE, JNTUA College of Engineering, Ananthapuramu., A.P., India.

Abstract

In recent years, wind power generation systems have increased installed capacity, requiring grid-connected inverters to control performance and impact output power quality and efficiency. In order to achieve optimal power factor and maintain a reasonable DC side bus voltage when handling direct-driven permanent magnet wind power, a grid-connected inverter is necessary. The stability of the DC side voltage in wind power systems affects the safety and stability of the system, as well as the independent management of the generator and grid converters. The architecture of the grid-connected inverter control system is crucial for wind power system control. Grid voltage variations and related loads can cause DC bus voltage fluctuations in wind power grid-connected inverters, which can seriously undermine the stability of the wind power system. To eliminate inverter DC bus voltage changes, we recommend combining fuzzy and neural network (NN) controllers with the enhanced linear active disturbance rejection controller (LADRC). In this study, the outer loop control is replaced with a linear active disturbance rejection control, which increases the reaction speed and reduces changes in the DC bus voltage. Software called MATLAB/SIMULINK will be used to implement the proposed system.

Keywords: Wind power inverter, LADRC, Neural network (NN), Fuzzy controller.

I. INTRODUCTION

Thanks to the rapid development and efficient use of high-power power electronic devices, one of the most widely used wind power generation models in China is the direct-drive permanent magnet wind generator set, which isolates the generator from the extensive power grid via a back-to-back dual pulse width modulation converter. One of the primary models of wind power generation in China is the direct-drive permanent magnet wind power generation system, which has become popular due to the quick development and effective application of high-power power electronic devices. The generator is isolated from the large power grid by the two pulse width modulation converters that are placed back-to-back [1]. For integrated system modeling and analysis, this research offers a modular admittance model for wind farms that is easily extensible. Additionally, wind farm wind turbine generator function depends on wind speed. Wind speed may continually change system stability. How to measure system stability over all wind speed operation space is equally difficult [2]. Wind power generating systems use grid-connected inverters for energy conversion. The disturbance has two basic components: Disturbance from converter internal parameters and external circumstances [3-4]. This work presents a regulator to manage the microgrid's inverter's dc-link voltage when circulating power.

A control algorithm activates in the event that the voltage surpasses the limit, a discharge resistor with a switch connected in series across the dc-link capacitor. In parallel-connected inverter case studies, small-signal analysis evaluates stability. A realistic low-voltage (LV) microgrid is also constructed and tested to evaluate the idea and regulator operations. Simulations show that the suggested regulator works under network disruptions [5-6]. replicates the effectiveness of the grid side inverter control method and analyzes it based on the grid voltage vector orientation, unit factor grid connection, and analysis [7]. Recommended replacing the standard PI controller with fuzzy and neural network PI controls to increase grid-connected current sine fullness and minimize harmonic content [8]. References [9, 10] describe how the DC side voltage is stabilized by reducing the grid side harmonic current using synovial variable structure control in the outer voltage loop and predictive current control in the inner loop.

This work studies microgrid inverter voltage management with modified rejection control for linear active disturbances (MLADRC). prolonged state observers measure filter capacitor current to indirectly calculate voltage error derivative, improving observation performance. The perturbation loop uses a first-order inertial connection to reduce observation noise. Nonlinear ADRC has been applied to an inverter in reference [11], but the controller design is complicated and has a lot of parameters; in reference [12], the output voltage error's differential term increased LESO's observer bandwidth, but the transformation caused LESO's parameters to double, making it challenging to set; and in reference [13], the LADRC of the reduce was suggested. A hybrid PMSG-based wind energy generating system with a novel FRT capability scheme is presented in this study. A fuzzy logic controller and brake chopper (BC) form the hybrid solution. FLC replaces all generator and grid side converter proportional-integral (PI) controllers. Additionally, a BC system is attached to the dc connection to increase PMSG dynamic reaction during faults [14]. This research presents enhanced A twin three-phase PMSG with deadbeat direct power control. By using deadbeat control of both active and reactive power, the active vector duty cycle is computed. This makes it possible for active and reactive power to match references as nearly as possible for the duration of each sample period. After that, a weight coefficient's effect on active and reactive power's steady-state performance is looked at [15]. One inverter using sinusoidal pulse width modulation (SPWM) that is driven by batteries excites the rotor. The suggested system charges/discharges batteries based on wind power to offer continuous power to the isolated load. The system functions in several modes depending on wind and load. This research discovered and documented all conceivable operating modes [16]. First-order inertial links have 10ms-15ms temporal constants.

There is a phase delay and amplitude offset between controller feedback and the actual bus voltage in the conventional voltage external loop second-order active disturbance rejection controller (ADRC) system because it disregards the bus voltage filter. Because of the first-order inertial link time constant, this will negatively impact system performance. In this work, the bus voltage filter is utilized to improve the ADRC [17]. Controller scaling frequency-scales an existing controller for a broad class of plants, reducing the repetitious controller tuning procedure for gain and bandwidth-different plants. Controller parameterization simplifies tuning by making controller parameters a function of the loop-gain bandwidth. Practical optimization maximizes bandwidth within physical limits, which limit performance [18-19]. [20] Suggested increasing the observer bandwidth to speed up RLESO tracking. He showed the second-order RLESO's error observation and filtering capabilities from both the time and frequency domains, emphasizing stability and anti-interference performance. However, he did not examine its speed, or more specifically, its dynamic observation performance. The results of the simulation validate the effectiveness of the method proposed in this study, and the frequency-domain analysis shows that the improved LADRC performs better in terms of interference than the regular LADRC.

II. MATHEMATICAL MODEL AND CONTROL STRATEGY OF GRID CONNECTED INVERTER

The power generating system with a direct-drive permanent magnet wind machine, seen in Figure 1, uses a rectifier on the machine side to convert the generator's output current which is subject to fluctuations due to the unpredictable wind speed into DC voltage, which is then stabilized by an intermediate DC voltage link.

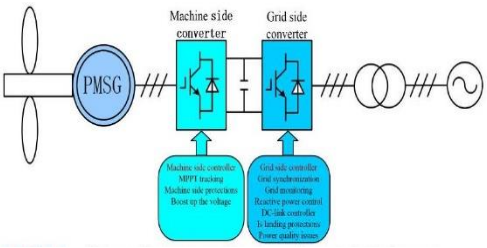

Figure 1. Schematic diagram of permanent magnet wind power generation system

Finally, the grid side inverter feeds the electricity into the power grid. To achieve optimal use of the generator's wind energy and accomplish by separating the generator's active and reactive power outputs, the generator's active power output can be controlled via the generator-side converter [14, 15].

In Figure 2, we can see the schematic of the grid-side inverter for the production of wind energy. The grid-side equivalent resistance is denoted by R_g in this picture, along with the grid-side filter's inductance (Lg), output voltages e_a, e_b, and e_c, the grid-side filter capacitor Cg, the bus filter capacitor C, and the DC bus voltage U_{dc}.

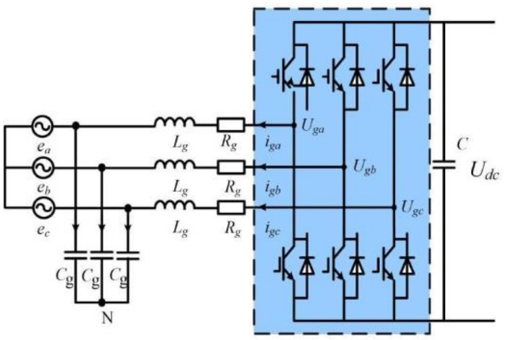

Figure 2. Overall control block diagram of wind power inverter

The following KVL three-phase voltage equation is derived based on the topology of the grid side inverter.

$$\begin{bmatrix} U_{ga} \\ U_{gb} \\ U_{gc} \end{bmatrix} = \begin{bmatrix} e_a \\ e_b \\ e_c \end{bmatrix} + R_g \begin{bmatrix} i_{ga} \\ i_{gb} \\ i_{gc} \end{bmatrix} + L_g \frac{d}{dt} \begin{bmatrix} i_{ga} \\ i_{gb} \\ i_{gc} \end{bmatrix} \quad (1)$$

$$\begin{bmatrix} i_{ga} \\ i_{gb} \\ i_{gc} \end{bmatrix} = \begin{bmatrix} i_a \\ i_b \\ i_c \end{bmatrix} + C_g \frac{d}{dt} \begin{bmatrix} U_{Ca} \\ u_{Cb} \\ u_{Cc} \end{bmatrix} \quad (2)$$

$$\begin{bmatrix} U_{gd} \\ U_{gq} \end{bmatrix} = \begin{bmatrix} e_d \\ e_q \end{bmatrix} + R_g \begin{bmatrix} i_{gd} \\ i_{gq} \end{bmatrix} + L_g \frac{d}{dt} \begin{bmatrix} i_{gd} \\ i_{gq} \end{bmatrix} + L_g \begin{bmatrix} -wi_{gq} \\ wi_{gd} \end{bmatrix} \quad (3)$$

$$\begin{bmatrix} i_{gd} \\ i_{gq} \end{bmatrix} = \begin{bmatrix} i_d \\ i_q \end{bmatrix} + C_g \frac{d}{dt} \begin{bmatrix} e_d \\ e_q \end{bmatrix} + \begin{bmatrix} -we_q \\ we_d \end{bmatrix} \quad (4)$$

In this context, U_{gd} and U_{gq} denote the grid-side inverter voltage, three-phase grid voltage, and grid-side inverter current components along the d and q axes, respectively. The d and q axis components of the output current are then indicated by the variables i_d and i_q, and lastly, w indicates the angular frequency of the grid output as determined by the phase-locked loop. The following can be derived by deriving and simplifying formula (3) and then replacing it with formula (2):

$$\frac{d^2}{dt^2} \begin{bmatrix} e_d \\ e_q \end{bmatrix} = \frac{1}{C_g L_g} \begin{bmatrix} U_{gd} \\ U_{gq} \end{bmatrix} - \frac{1}{C_g L_g} \begin{bmatrix} e_d \\ e_q \end{bmatrix} - \frac{R_g}{C_g L_g} \begin{bmatrix} i_{gd} \\ i_{gq} \end{bmatrix} + \frac{1}{C_g} \begin{bmatrix} wi_{gq} \\ -wi_{gd} \end{bmatrix} - \frac{d}{C_g dt} \begin{bmatrix} i_d \\ i_q \end{bmatrix} + \frac{d}{C_g dt} \begin{bmatrix} we_q \\ -we_d \end{bmatrix} \quad (5)$$

Since the grid-side inverter for wind power is a tightly connected system with several variables, as shown in equation (5), conventional control procedures are inadequate for meeting industry requirements for control. An inner loop for current and an outer loop for voltage make up the voltage-oriented vector control scheme used by the majority of grid-connected inverters [17]. With the help of this control mode, the inverter may meet grid connection requirements for unity power factor while preserving the stability of the DC side voltage and generating a high-quality sinusoidal current waveform on the AC side. The goal of maintaining voltage stability can be achieved by modifying the management of the voltage outer loop in accordance with the difference between the supplied DC side voltage and the feedback. The major purpose of the current inner loop is to accelerate the provided; the d-axis current is the output of this loop. As seen in Figure 3, there are vector diagrams in the $e_d=|E|$, $e_q=0$, α-β, and d-q coordinate systems, which must be aligned with the grid voltage space vector E during the coordinate transformation process. This means that the zero point of the rotation angle Θ is taken as the peak of phase an of the grid voltage.

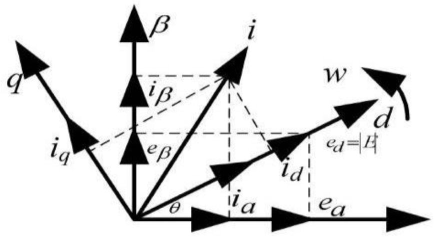

Figure 3. The grid-side voltage and current vector diagrams in α-β and d-q coordinate systems

In Figure 3, i_d and i_q are the active and reactive components in the side currents respectively; u_d, u_q are the output's control quantities. Considering that in a steady-state i_d and i_q are both direct current, and since their differential term is zero, we may obtain the following using formula (3):

$$\begin{cases} U_d = e_d - R_g i_d + wLi_q \\ U_q = -R_g i_q - wLi_d \end{cases} \quad (6)$$

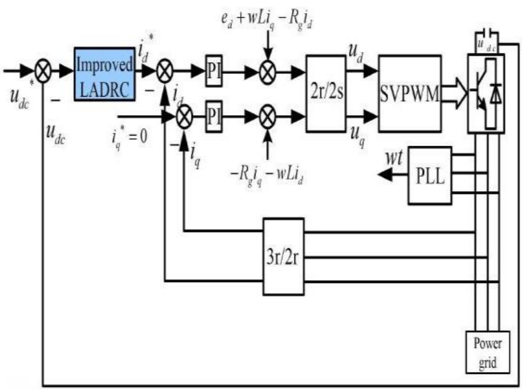

Figure 4. Grid side inverter grid voltage vector directional control block diagram

In order to maintain the stability of the DC bus voltage in the double closed-loop structure, take into account the output of the voltage outer loop as the given value of the active current of the current inner loop; the reactive current is given externally and set to zero to realize unity power factor grid connection [18]. To get the control variables u_d and u_q, the current inner loop is used to feed back the active and reactive currents. Then, the closed-loop output is applied to the steady-state control equation. As shown in the picture

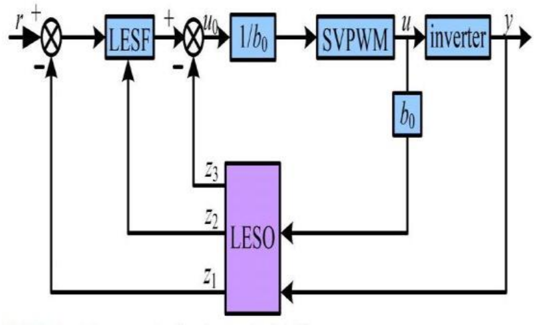

Figure 5. The overall structure of LADRC

below, the grid-side inverter may be turned on and off using the control quantities u_d and u_q, whose interface is connected to the space vector pulse width modulation technique. Figure 4 depicts the voltage-oriented vector control block diagram for grid-side inverters.

III. METHODOLOGY

Linear Active Disturbance Rejection Controller (LADRC)

Figure 5 shows that traditional LADRC has three parts: The three components that control the transition process are the linear state error feedback rate (LSEF), linear extended state observer (LESO), and linear tracking differentiator (LTD). They also remove rapidity and overshoot [19], extract the differential signal, and stop bus voltage oscillation. LTD is not used in this article.

Fuzzy Logic Controller

The Fuzzy Logic controller (FLC) in this paper is used to manage the effect of voltage disturbances in the wind power system. In this paper, FLC is applied under two conditions i.e., at 30% and 40% of symmetrical and asymmetrical drop failures, where its performance is analyzed based on DC side bus voltage waveforms.

In addition to providing accurate results, Fuzzy Logic Controllers are simple, adaptable, and resilient, making them ideal for solving difficult situations. Hence, the system's responsiveness will be enhanced. MATLAB/Simulink is used to assess the outcomes of this system's simulations. While FLC's installation is simple to plan, its application is more challenging due to the need for qualitative understanding.

Neural Network Controller

The Neural Network (NN) Controller in this paper used to manage the effect of voltage disturbances in the wind power system, like the Fuzzy Logic Controller. NN controller is also applied under two conditions i.e., at 30% and 40% of symmetrical and asymmetrical drop failures, where its performance is analyzed based on DC side bus voltage waveforms.

A neural network (NN) controller is a kind of control system that makes judgments and manages a system or process using artificial neural networks. This is a control engineering application of neural networks. In a neural network controller, the neural network learns to map sensory inputs from the system to appropriate control actions in order to achieve a desired output. The inputs can be from sensors that measure temperature, pressure, or other parameters, while the output could be a control signal to adjust a valve, motor, or other components.

The neural network controller is trained on a dataset of input-output pairs, which helps it to become familiar with the connections between the signals being input and output. When the controller is trained, can make decisions and adjust its outputs in real-time based on the current input signals. Neural network controllers have found widespread use in various fields, such as robotics, process control, and autonomous vehicles, where they are used to make decisions and control systems based on sensor inputs. They have the potential to improve system performance and efficiency and can adapt to changing conditions and environments.

IV. RESULTS AND DISCUSSION

A.SYMMETRICAL DROP FAILURE

30%

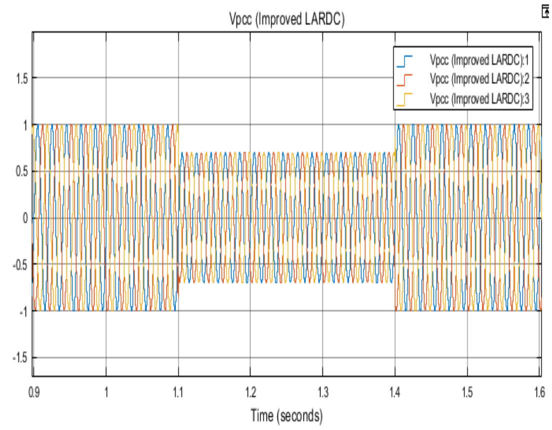

(a)

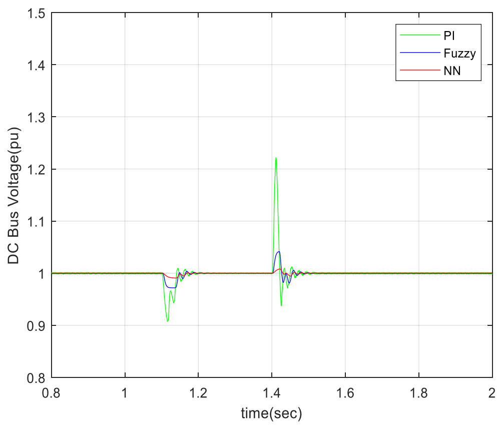

(b

Figure 6: The voltage waveform of the busbar under the condition of symmetrical drop of 30% of the grid voltage; (a) Grid connected point voltage; (b) Symmetrical drop bus voltage

The grid linked point voltage, as shown in Figure 6(a), of LADRC of all three phases as displayed. Figure 6(b) shows the DC bus voltage of PI controller fluctuates from 0.91 to 1.22 pu. In Fuzzy controller, it fluctuates from 0.97 to 1.03 pu. In case of neural network controller, it fluctuates from 0.99 to 1.01 pu. By comparing three controllers, we can see that the LADRC of neural network controller has the less fluctuations and it can get to a steady condition of 1.0 pu.

B. ASYMMETRIC DROP FAILURE 30%

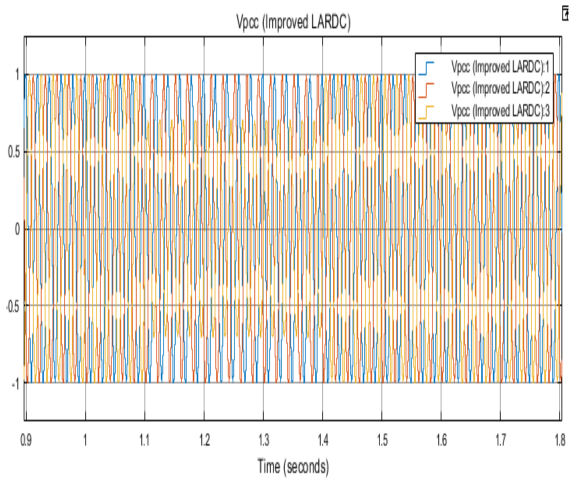

(a)

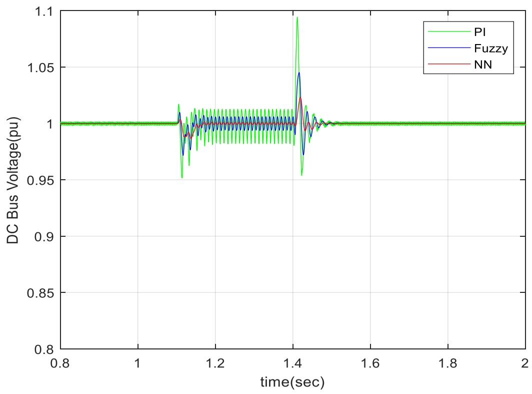

(b)

Figure 7: The voltage waveform of the busbar under the condition of 30% asymmetrical drop of the grid voltage; (a) Grid-connected point voltage; (b) Asymmetric drop bus voltage

When the grid voltage is lowered asymmetrically, Figure 7 displays the waveforms of the grid voltage and DC bus voltage. When configured to 1.1s, when an asymmetrical drop failure in grid voltage transpires, the drop amplitude is 30%, and it returns to normal after 0.3s. from Figure 7(b), the DC bus voltage of the LADRC of neural network controller has the smaller fluctuation range as compared to other controllers.

C.MOTOR LOADING AND UNLOADING 30%

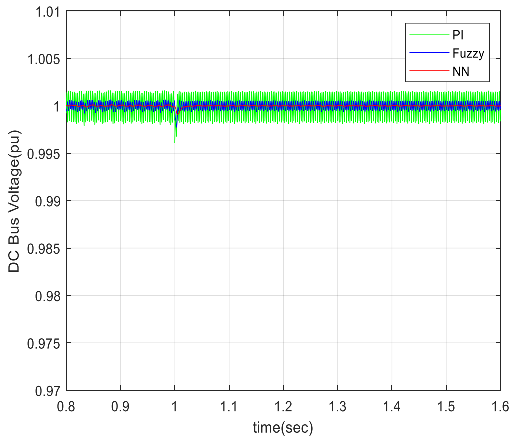

(a)

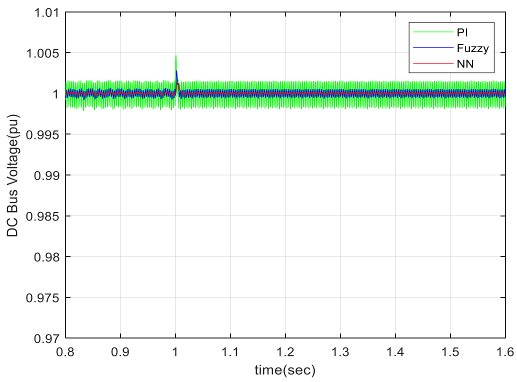

(b)

Figure 8: The bus voltage of the motor under load and unload conditions; (a) Motor load 30%; (b) Motor load reduction 30%

When the motor is loaded and unloaded, Figure 8 displays the DC bus voltage waveform of the grid-connected inverter. Figure 8(a) illustrates the variation in DC bus voltage at 30% motor load. It is evident that the PI, Fuzzy, and Neural Network controllers cause overshoots in DC bus voltage. By comparing these controllers, we can see that the neural network controller has the better stable performance and it can quickly reach to 1.0 pu. Figure 8(b), shows When the motor load is lowered by 30%, the DC bus voltage changes, and it is evident that the neural network controller of the LADRC controls the DC bus voltage with a drop amplitude that has superior performance stability.

D. SYMMETRICAL DROP FAILURE 40%

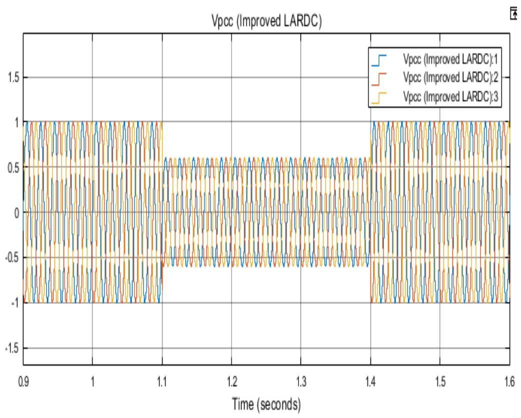

(a)

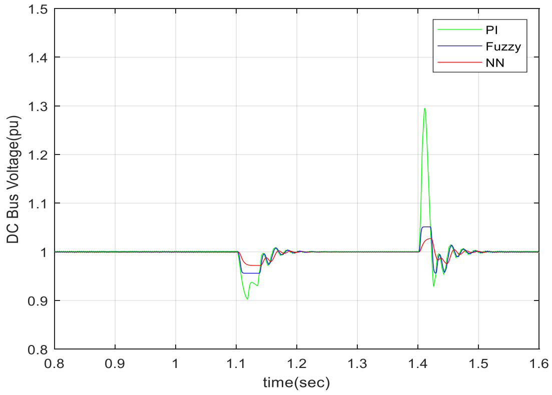

(b)

Figure 9: The voltage waveform of the busbar under the condition of symmetrical drop of 40% of the grid voltage; (a) Grid connected point voltage; (b) Symmetrical drop bus voltage

From figure 9, In the event of a 40% grid voltage symmetrical drop, it displays the waveforms for the grid voltage and the DC bus voltage. The grid voltage has a symmetrical 40% drop when the setting is set to 1.1 seconds, and it recovers to normal in 0.3 seconds. When a fault arises, based on Figure 9(b), the overshoot of DC bus voltage controlled by PI controller fluctuates from 0.91 pu to1.29 pu and Fuzzy controller fluctuates from 0.96 pu to 1.05 pu and the neural network controller fluctuates from 0.98 to 1.03 pu. As compared with PI and Fuzzy, NN controller of LADRC can reach the steady stable state and has better stability.

E. ASYMMETRIC DROP FAILURE 40%

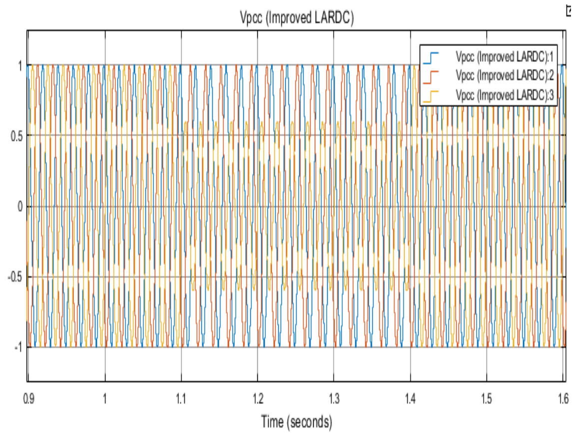

(a)

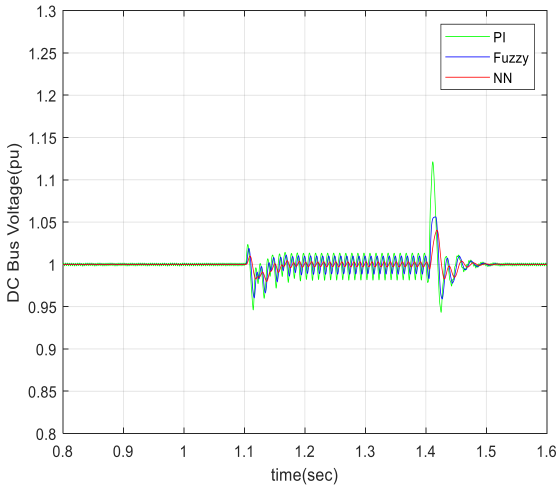

(b)

Figure 10: The voltage waveform of the busbar under the condition of 40% asymmetrical drop of the grid voltage; (a) Grid-connected point voltage; (b) Asymmetric drop bus voltage

From figure 10, an uneven decline in the grid voltage of waveforms are shown. When There is an uneven 40% decline in grid voltage The neural network controller of LADRC's DC bus voltage has a superior control effect on the DC bus voltage stability in the presence of disturbances.

F. MOTOR LOADING AND UNLOADING 40%

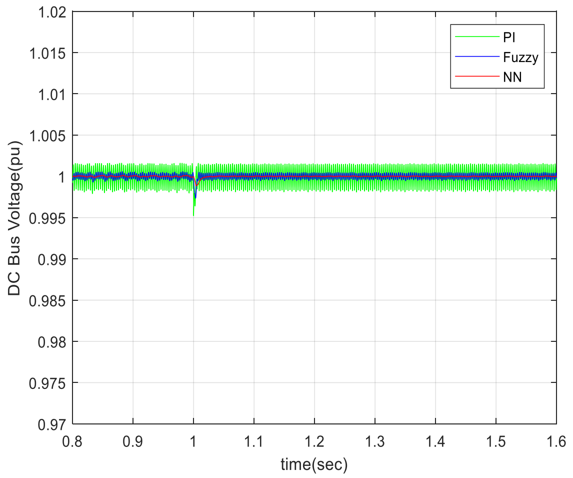

(a)

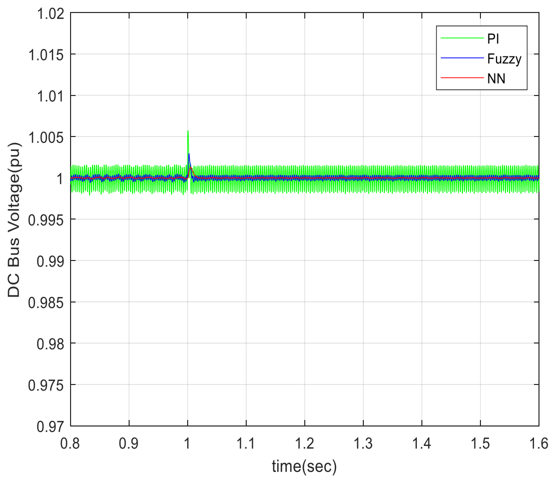

(b)

Figure 11: The bus voltage of the motor under load and unload conditions; (a) Motor load 40%; (b) Motor load reduction 40%.

From Figure 11(a) & (b), When the motor is loaded and its voltage is lowered by 40%, the DC bus voltage fluctuates. It is evident that the NN, PI, and fuzzy controllers are in charge of regulating these excursions. By comparison of controllers, we can see that the LADRC of neural network controller has good stability and smaller fluctuation range during the loading and unloading of the motor.

V. CONCLUSION

By addressing the limitations of conventional LADRC of PI controller, we were able to develop a more effective LADRC voltage outer loop of Fuzzy and Neural network (NN) controllers that significantly enhanced the grid-connected inverter's DC side voltage stability for direct-drive permanent magnet wind power generation. The DC bus and voltage response speed voltage fluctuations are both dramatically improved by the Neural Network (NN) controller as compared to other controllers according to the simulation findings. Even when subjected to environmental disturbances, the developed controller outperforms the conventional LADRC of PI controller in terms of control effect and increases the wind energy consumption rate. The simulation experiment further validated the controller's efficacy. This study presents an enhanced LADRC controller that offers a novel approach to controlling grid-connected inverters for wind generation, which has practical engineering applications.

REFERENCES

[1] S. Lei, Research on Control Technology of Grid-Connected Inverter for 1.5 MW Wind Turbines, Changchun, China: Changchun Univ. Technology, 2018.

[2] X. Zou, X. Du and H. Tai, "Stability analysis for direct-drive permanent magnet synchronous generator based wind farm integration system considering wind speed", IET Renew. Power Gener., vol. 14, no. 11, pp. 1894-1903, Aug. 2020.

[3] W. Xuan, Research on Linear Active Disturbance Rejection Control Strategy of Three-level PWM Rectifier, Xi'an, China:Xi'an Univ. Technology, 2018.

[4] L. Ping and W. Jiuhe, "Research on control strategy of Vienna rectifier based on passive and active disturbance rejection", Power Grid Technol., pp. 1-12, Dec. 2021.

[5] L. Xinrui, G. Chao and W. Zhiliang, "DC bus voltage control of photovoltaic grid-connected inverter based on nonlinear disturbance observer", Power Syst. Technol., vol. 44, no. 3, pp. 897-906, 2020.

[6] M. A. Hossain, H. R. Pota, A. M. O. Haruni and M. J. Hossain, "DC-link voltage

regulation of inverters to enhance microgrid stability during network contingencies", Electr. Power Syst. Res., vol. 147, pp. 233-244, Jun. 2017.
[7] G. Jin, W. Lei and L. Yi, "Research on grid-connected inverter of permanent magnet direct drive variable speed constant frequency wind power system", Power Electron., vol. 51, no. 10, pp. 24-26, 2017.
[8] F. Diansen, Research on the Control Technology of Wind Power Grid-Connected Inverter, Zhuzhou, China:Hunan Univ. Technology, 2018.
[9] W. Guixin and J. Shenyi, "Research on control strategy based on three-phase voltage type PWM rectifier", Elect. Drive, vol. 49, no. 10, pp. 34-38, 2019.
[10] T. Meng, Z. Bowen, Z. Lawu, Y. Hongzhi and L. Yan, "Research on sliding mode variable structure independent pitch control based on RBF neural network", Power Syst. Protection Control, vol. 47, no. 4, pp. 107-114, 2019.
[11] Z. Zubing, C. Lijuan and G. Huixia, "Active disturbance rejection control strategy of voltage source PWM inverter", J. Electrotechnics, vol. 2, pp. 84-88, Jan. 2004.
[12] Y. Lin, Z. Jiang, M. Wenjie and H. Zhonglong, "Voltage control of microgrid inverter based on improved second-order linear auto-disturbance rejection technology", Automat. Electr. Power Syst., vol. 43, no. 4, pp. 146-153, 2019.
[13] Wang Chunyang, Zhao Shangqi, Shi Hongwei, Liu Xuelian. Linear Active Disturbance Rejection Control of Airborne Optoelectronic Stabilized Aiming Platform[J]. Infrared and Laser Engineering, 2019, 48(12):248-254.
[14] M. Metwally Mahmoud, H. S. Salama, M. M. Aly and A.-M.-M. Abdel-Rahim, "Design and implementation of FLC system for fault ride-through capability enhancement in PMSG-wind systems", Wind Eng., vol. 45, no. 5, pp. 1361-1373, Oct. 2021.
[15] S. Jin, W. Zhao, J. Ji and D. Xu, "Deadbeat direct power control for dual three-phase PMSG used in wind turbines", IET Renew. Power Gener., vol. 15, no. 9, pp. 1976-1984, Jul. 2021.
[16] K. Vijayakumar, N. Kumaresan and N. A. Gounden, "Operation and closed-loop control of wind-driven stand-alone doubly-fed induction generators using a single inverter-battery system", IET Electr. Power Appl., vol. 6, no. 3, pp. 162-171, 2012.
[17] X. Zhou, M. Liu, Y. Ma and S. Wen, "Improved linear active disturbance rejection controller control considering bus voltage filtering in permanent magnet synchronous generator", IEEE Access, vol. 8, pp. 19982-19996, 2020.
[18] L. Jie, Q. Xiaohui, W. Hui and X. Yuanqing, "Active disturbance rejection control: Summary and prospects of research results", Control Theory Appl., vol. 34, no. 3, pp. 281-295, 2017.
[19] Z. Gao, "Scaling and bandwidth-parameterization based controller tuning", Proc. Amer. Control Conf., pp. 4989-4996, Jun. 2003.
[20] Y. Dong, M. Xiaojun, Z. QingHan and Q. Xiaobo, "Research on frequency band characteristics and parameter configuration of linear ADRC for second-order systems", Control Theory Appl., vol. 30, no. 12, pp. 1630-1640, 2013.
[21] . Dong, M. Xiaojun, Z. Qinghan and Q. Xiaobo, "Study on frequency band characteristics and parameter configuration of linear active disturbance rejection controller for second-order